Supporting Information

for

Surface Chemistry Tuned Cellulose Nanocrystals in Bentonite Suspension for Water-based Drilling Fluids

Mei-Chun Li[1], Suxia Ren[2], Xiuqiang Zhang[2], Lili Dong[2], Tingzhou Lei[2], Sunyoung Lee[3], and Qinglin Wu[1,*]

[1] School of Renewable Natural Resources, Louisiana State University AgCenter, Baton Rouge, Louisiana 70803, United States

[2] Key Biomass Energy Laboratory of Henan Province, Zhengzhou, 450008, Henan, China

[3] Department of Forest Products, National Institute of Forest Science, Seoul 130-712, Korea

[*]Corresponding Author:

Qinglin Wu. E-mail: wuqing@lsu.edu

Supporting information consists of 14 pages, 9 Figures and 2 Tables.

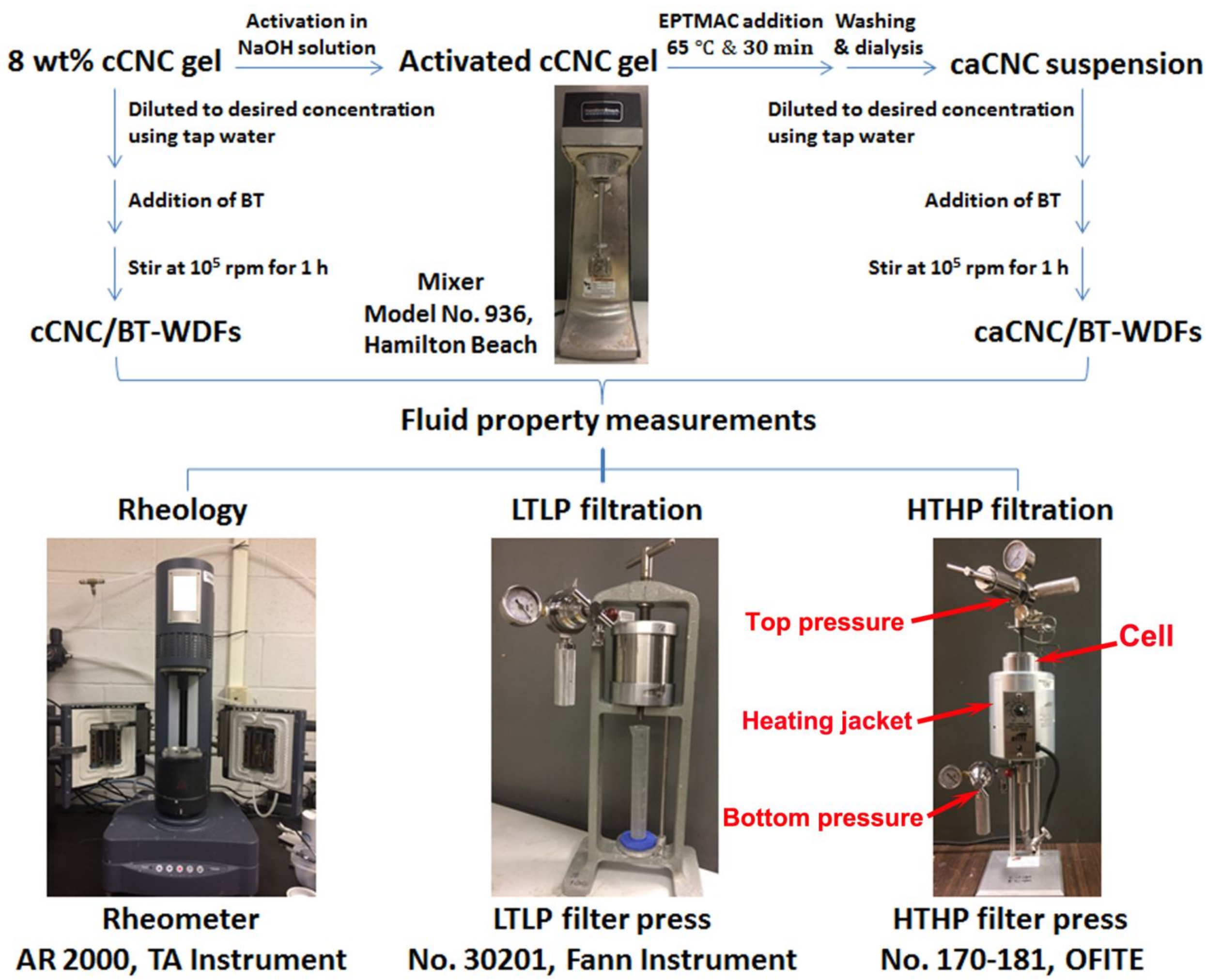

Figure S1. Flow chart for the formulation and characterization of CNC/BT-WDFs.

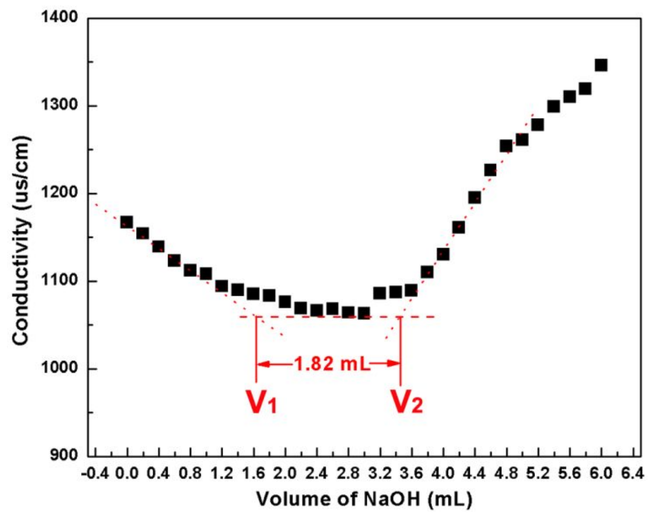

Figure S2. Typical conductometric titration curve of cCNCs.

The content of carboxyl group (C_{cg}) was calculated using the following equation:[1]

$$C_{cg} = \frac{(V_2 - V_1) \times C}{m - 36 \times (V_2 - V_1) \times C} \qquad (1)$$

where V_2 and V_1 are the equivalent volume of NaOH in L shown in Figure S2, c is the concentration of NaOH in mol/L, and m is the mass of CNCs used for conductometric titration.

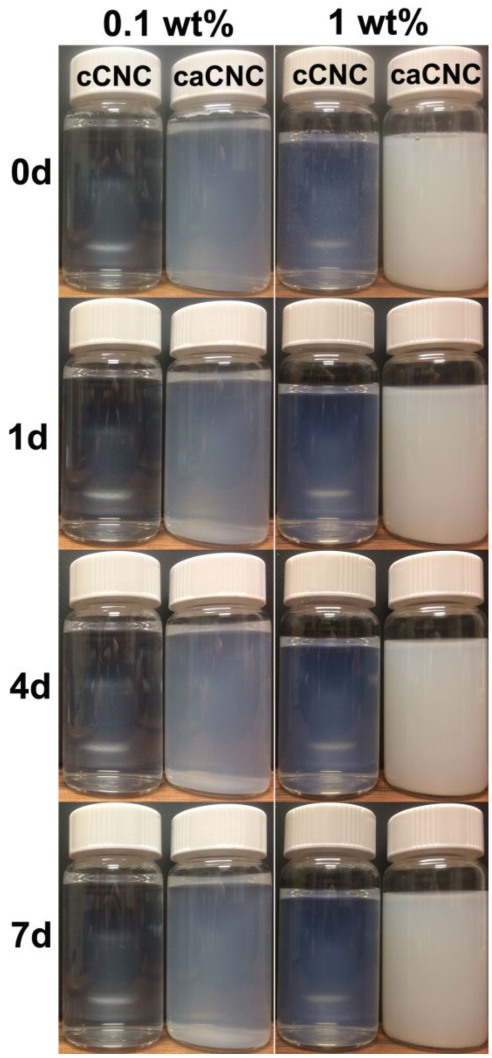

Figure S3. Appearance and static precipitation phenomena of cCNC and caCNC suspensions at concentrations of 0.1 and 1 wt% for 0, 1, 4 and 7 days.

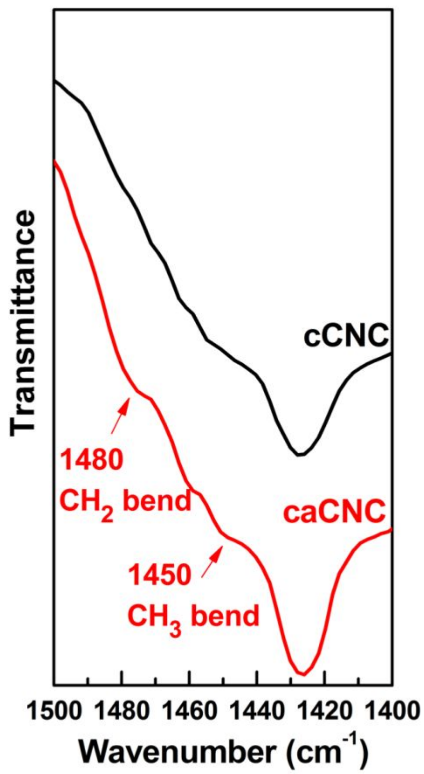

Figure S4. Enlarged FTIR spectra of cCNCs and caCNCs in the wavenumber range from 1400 to 1500 cm^{-1}.

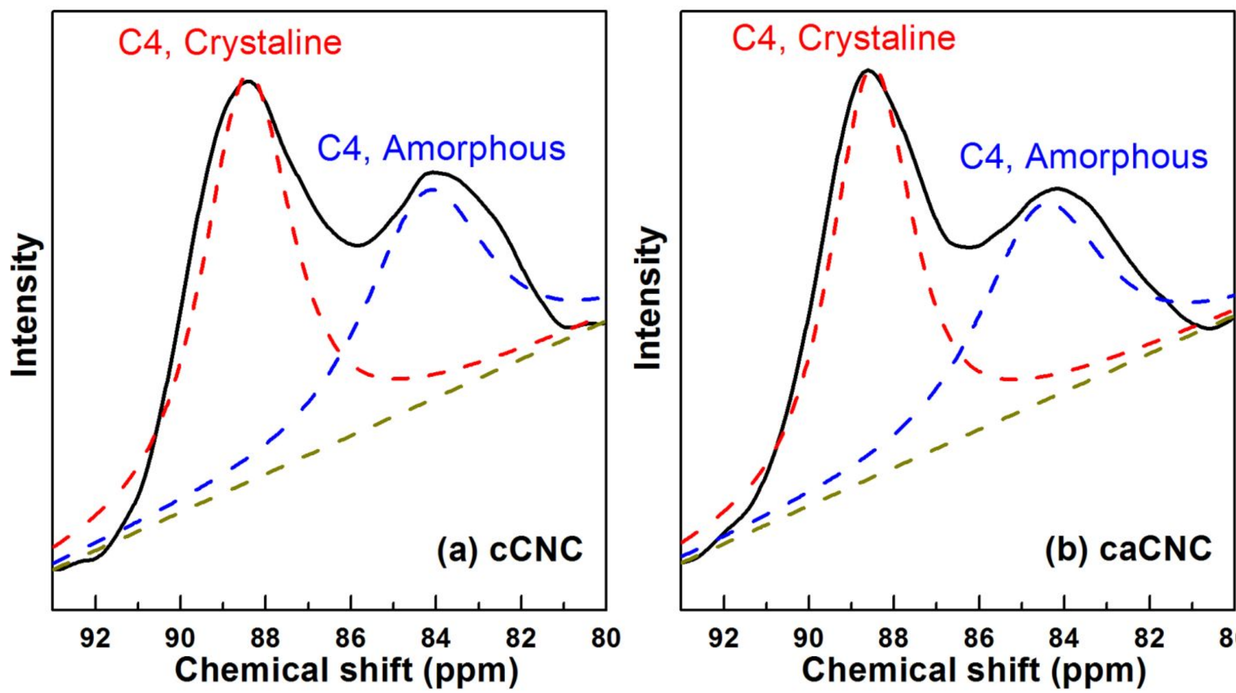

Figure S5. Deconvolution of C4 region from 80 to 93 ppm into two peaks centered at 84.1 and 88.4 ppm for (a) cCNCs and (b) caCNCs.

The crystallinity index (CI) was calculated using the following equation:[2]

$$\mathrm{CI} = \frac{A_1}{A_1 + A_2} \times 100\% \qquad (2)$$

where A_1 and A_2 the area of crystalline and amorphous domains, respectively.

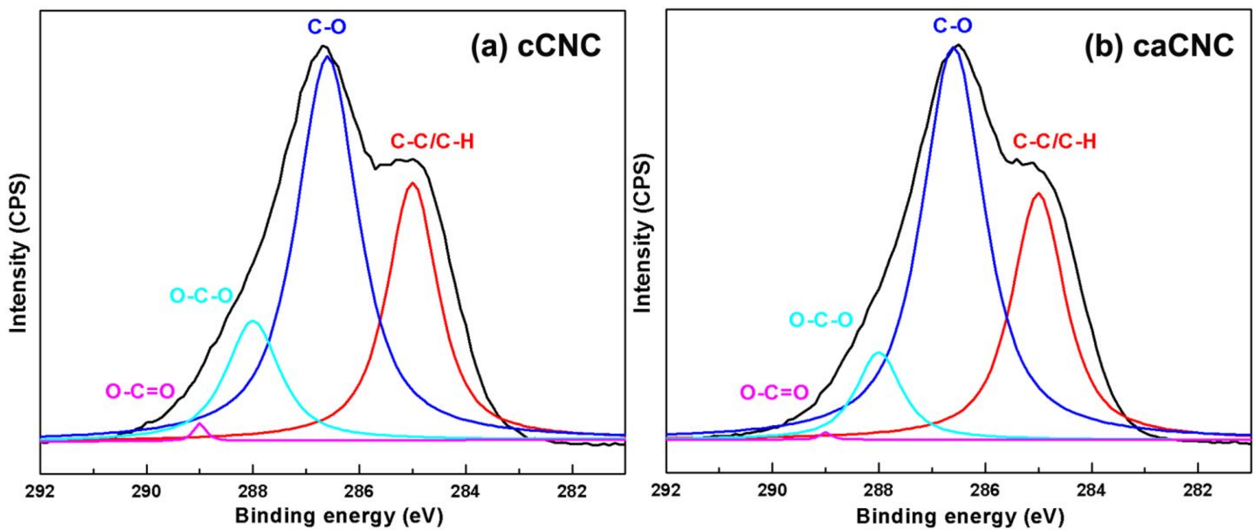

Figure S6. Deconvolution of the high-resolution C 1s peak for (a) cCNCs and (b) caCNCs.

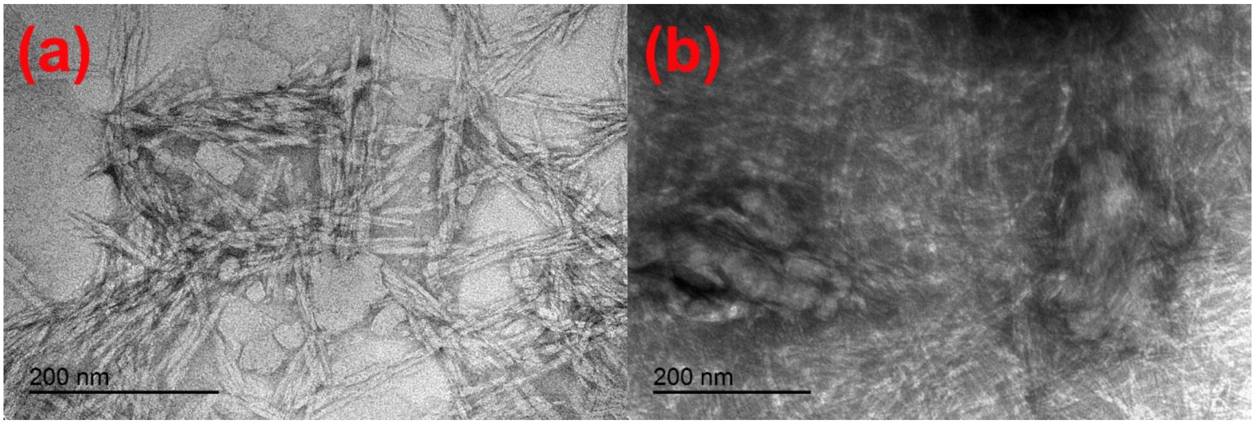

Figure S7. TEM micrographs of highly diluted CNC/BT-WDFs: (a) cCNC/BT and (c) caCNC/BT.

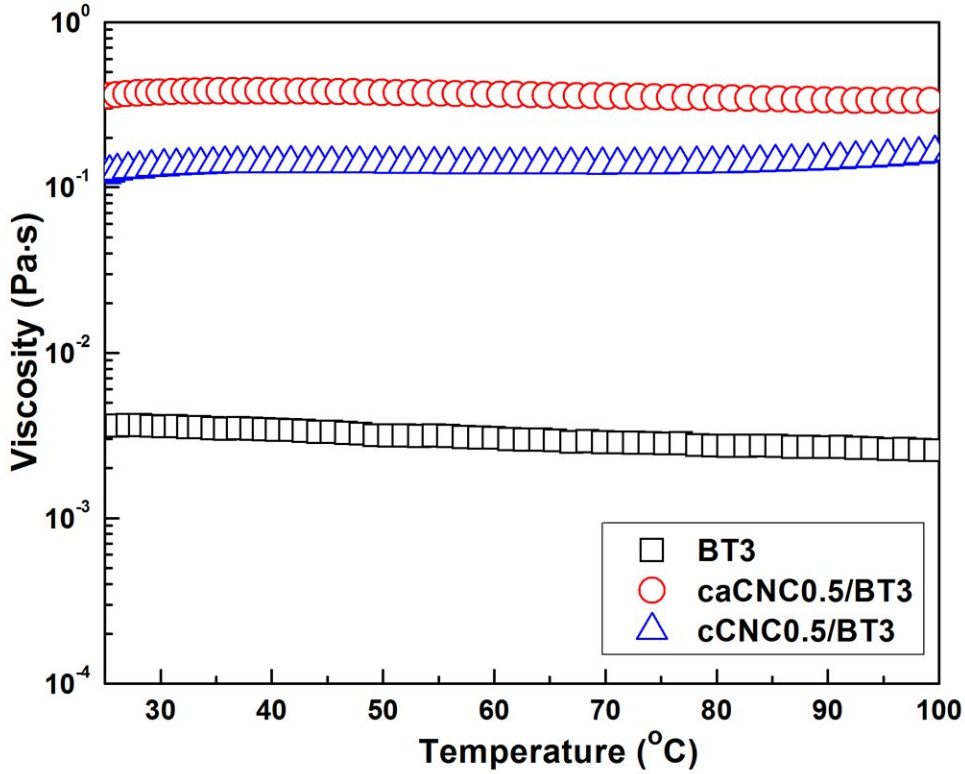

Figure S8. Shear-state viscosity of BT and CNC/BT-WDFs as a function of temperature range from 25 to 100 °C. The shear rate was fixed at 10 s^{-1}.

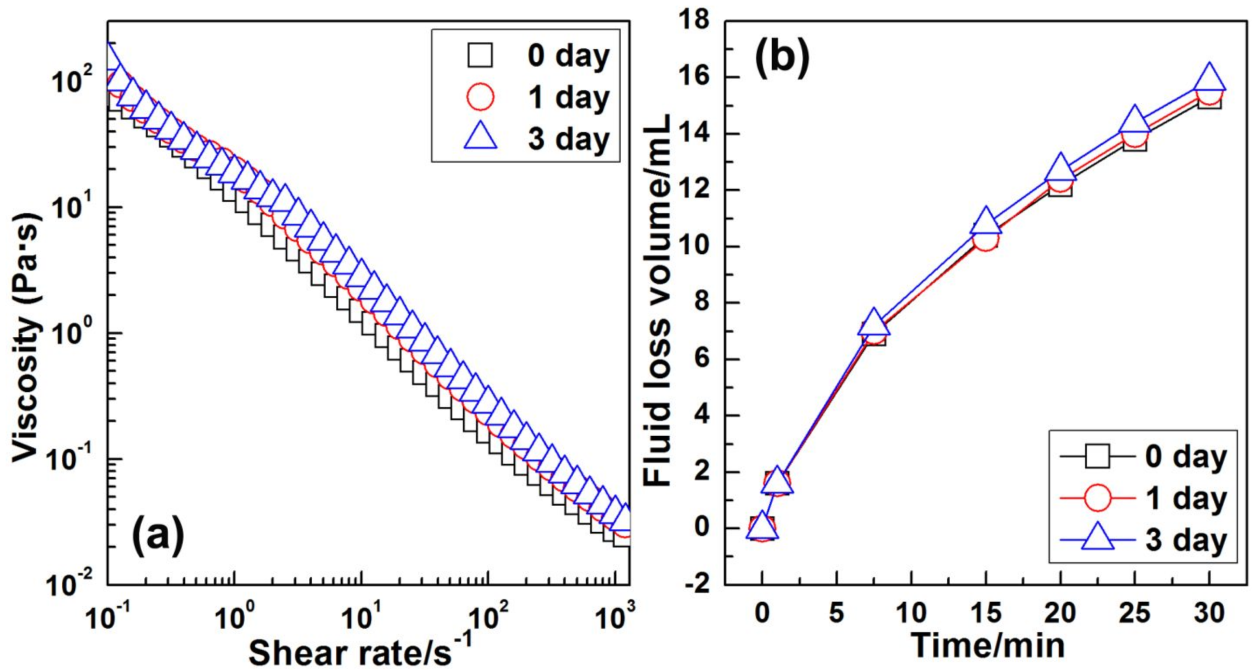

Figure S9. Influence of aging time on (a) rheological and (b) filtration performance of cCNC2/BT3-WDFs.

Table S1. Atomic surface composition from wide scan and quantification of differently bonded carbon atoms from C 1s high-resolution scan for cCNCs and caCNCs.

Sample	Atomic composition (%)			O/C	Bonded carbon composition (%)			
	C	N	O		C-C/H	C-O	O-C-O	O-C=O
cCNCs	66.81	-	33.19	0.50	30.14	54.54	14.79	0.53
caCNCs	72.12	0.64	27.24	0.39	31.34	58.96	9.48	0.22

The method used to determine the content of EPTMAC in caCNCs (mmol/g) is given as below:

1) The N atomic composition in caCNCs is determined as 0.64 % through XPS analysis with the SpecLab software.
2) The N atomic composition in caCNCs can be also written in the following form:

$$N\% = \frac{Num_N}{Num_C + Num_O + Num_N} \times 100\% = 0.64\% \qquad (3)$$

where Num_C, Num_O, and Num_N represent the number of carbon, oxygen and nitrogen in caCNCs, respectively.

3) If we denote the molarity of EPTMAC substituent on the surface of caCNC as X, and the molarity of anhydroglucose units (AGU) in caCNC as Y, then the molecular formula of caCNCs can be written in the form of (C6H10O5)Y-(C6H14ONCl)X. Consequently, the Equation 3 can be written as:

$$N\% = \frac{X}{(6Y + 6X) + (5Y + 1X) + 1X} \times 100\% = 0.64\% \qquad (4)$$

After reorganization, the X/Y ratio value for caCNCs (i.e., substitution degree in mol/mol) is obtained as ~ 0.07 mol/mol.

4) The AGU unit has the molar mass of 162.14 g/mol. Therefore, the content of EPTMAC in caCNCs (mmol/g of AGU) can be calculated through dividing 0.07 mol/mol by 162.15 g/mol, which gives 0.43 mmol/g.

Table S2. Comparison on the effectiveness of different nanoparticles at the same concentration of 0.5 wt% in improving rheological and filtration performance of BT-WDFs under LTLP conditions.

Nanoparticles	Particle size (nm)	C_r	C_f	References
SiO_2	5-20	0.24	0.07	3
Clay/SiO2 hybrid	1-5	0.58	0.46	
Fe_2O_3	3	1.34	-0.11	4
Fe_2O_3	30	0.95	-0.02	
Fe_2O_3/Clay hybrid	N/A	8.47	0.36	
Al_2O_3/SiO_2/Clay hybrid	N/A	-0.76	0.19	
ZnO	< 50	0.30	N/A	5
CuO	< 50	0.72	N/A	
Colloidal SiO_2	9.5	0.5	0.95	6
Powder SiO_2	N/A	0.13	0.47	
SiO_2	N/A	2.32	N/A	7
Carbon nanotube	N/A	1.41	N/A	
ZnO	< 20	0.82	N/A	
Carbon nanotube/SiO_2	N/A	1.55	N/A	
SiO_2	5	2.94	N/A	8
SiO_2	10	1.11	N/A	
SiO_2	50	0.02	N/A	
TiO_2	47	1.85	N/A	
Al_2O_3	43	1.32	N/A	
Starch	920-7000	1.33	0.63	9
Sulfated CNCs	width 6.1 $\pm$ 3.5 length 228.4 $\pm$ 63.8 aspect ratio ~37	91.19	0.31	10
CNFs	width 12.5 $\pm$ 8.4 length > 1000 aspect ratio > 80	34.94	-0.05	
Carboxylated CNCs	width 9–14 length 100–150 aspect ratio ~10	52.75	0.18	This study

Two coefficients C_r and C_f are adopted to represent the effectiveness of nanoparticles on the rheological and filtration performance of BT-WDFs, respectively; which are calculated based on the following two Equations:

$$C_r = \frac{YS_{filled} - YS_{control}}{YS_{control}} \quad (5)$$

$$C_f = \frac{FL_{control} - FL_{filled}}{FL_{control}} \quad (6)$$

where $YS_{control}$, YS_{filled}, $FL_{control}$ and FL_{filled} are yield stress and fluid loss of neat BT-WDFs (i.e., control sample) and nanoparticles filled BT-WDFs, respectively. The higher the coefficients are, the more effectiveness the nanoparticles in improving the performance of BT-WDFs.

REFERENCES

(1) da Silva Perez, D.; Montanari, S.; Vignon, M. R. TEMPO-Mediated Oxidation of Cellulose III. *Biomacromolecules* **2003**, *4*, 1417–1425.

(2) Park, S.; Baker, J. O.; Himmel, M. E.; Parilla, P. A.; Johnson, D. K. Cellulose crystallinity index: measurement techniques and their impact on interpreting cellulase performance. *Biotechnol. Biofuels* **2010**, *3*, 10.

(3) Cheraghian, G.; Wu, Q.; Mostofi, M.; Li, M.-C.; Afrand, M.; S.Sangwai, J. Effect of a novel clay/silica nanocomposite on water-based drilling fluids: Improvements in rheological and filtration properties. *Colloids Surfaces A Physicochem. Eng. Asp.* **2018**, *555*, 339–350.

(4) Barry, M. M.; Jung, Y.; Lee, J.-K.; Phuoc, T. X.; Chyu, M. K. Fluid filtration and rheological properties of nanoparticle additive and intercalated clay hybrid bentonite drilling fluids. *J. Pet. Sci. Eng.* **2015**, *127*, 338–346.

(5) William, J. K. M.; Ponmani, S.; Samuel, R.; Nagarajan, R.; Sangwai, J. S. Effect of CuO and ZnO nanofluids in xanthan gum on thermal, electrical and high pressure rheology of water-based drilling fluids. *J. Pet. Sci. Eng.* **2014**, *117*, 15–27.

(6) Ghanbari, S.; Kazemzadeh, E.; Soleymani, M.; Naderifar, A. A facile method for synthesis and dispersion of silica nanoparticles in water-based drilling fluid. *Colloid Polym. Sci.* **2016**, *294*, 381–388.

(7) Sadegh Hassani, S.; Amrollahi, A.; Rashidi, A.; Soleymani, M.; Rayatdoost, S. The effect of nanoparticles on the heat transfer properties of drilling fluids. *J. Pet. Sci. Eng.* **2016**, *146*, 183–190.

(8) Minakov, A. V; Zhigarev, V. A.; Mikhienkova, E. I.; Neverov, A. L.; Buryukin, F. A.; Guzei, D. V. The effect of nanoparticles additives in the drilling fluid on pressure loss and cutting transport efficiency in the vertical boreholes. *J. Pet. Sci. Eng.* **2018**, *171*, 1149–1158.

(9) Zoveidavianpoor, M.; Samsuri, A. The use of nano-sized Tapioca starch as a natural water-soluble polymer for filtration control in water-based drilling muds. *J. Nat. Gas Sci. Eng.* **2016**, *34*, 832–840.

(10) Li, M.-C.; Wu, Q.; Song, K.; Qing, Y.; Wu, Y. Cellulose Nanoparticles as Modifiers for Rheology and Fluid Loss in Bentonite Water-based Fluids. *ACS Appl. Mater. Interfaces* **2015**, *7*, 5006–5016.